Mass and width of the $\Upsilon(4S)$

Eef van Beveren [1] and George Rupp [2]

[1] *Centro de Física Computacional, Departamento de Física, Universidade de Coimbra, P-3004-516 Coimbra, Portugal*
eef@teor.fis.uc.pt

[2] *Centro de Física das Interacções Fundamentais, Instituto Superior Técnico, Universidade Técnica de Lisboa, Edifício Ciência, P-1049-001 Lisboa, Portugal*
george@ist.utl.pt

PACS number(s): 14.40.Gx, 13.25.Gv, 14.40.Nd, 11.80.Gw

October 6, 2009

Collaboration for the Resonance-Spectrum Expansion

Abstract

Recent data on $e^-e^+ \to b\bar{b}$ by the *BABAR* Collaboration [B. Aubert *et al.*, Phys. Rev. Lett. **102**, 012001 (2009)] in the energy range delimited by the $B\bar{B}$ and $\Lambda_b\bar{\Lambda}_b$ thresholds are analyzed in a multichannel formalism that incorporates the usual Breit-Wigner resonances, but interfering with a background signal due to the opening of open-bottom thresholds. In particular, the $\Upsilon(4S)$ resonance is determined to have a mass of 10.735 GeV and a width of 38 MeV. Also two higher Υ resonances are identified, parametrized, and classified.

Moreover, it is found that near the $B\bar{B}$ threshold open-bottom production in electron-positron annihilation is dominated by the reaction chain $e^-e^+ \to n\bar{n} \to B\bar{B}$ ($n = u/d$) rather than $e^-e^+ \to b\bar{b} \to B\bar{B}$, whereas near the $B_s\bar{B}_s$ threshold the reaction chain $e^-e^+ \to s\bar{s} \to B\bar{B}$ dominates the production amplitude.

The vital role played in this analysis by the *universal confinement frequency* ω, defined in 1980 [E. van Beveren, C. Dullemond, and G. Rupp, Phys. Rev. D **21**, 772 (1980)] and accurately determined in 1983 [E. van Beveren, G. Rupp, T. A. Rijken, and C. Dullemond, Phys. Rev. D **27**, 1527 (1983)], is further confirmed.

1 Introduction

In recent years, several experimental groups, in particular the *BABAR* Collaboration, have published data that were only partly analyzed, thus offering us the opportunity to also interpret measurements outside the invariant-mass regions of direct interest for these experiments. We welcome this attitude, since it supplies us with valuable pieces of information, allowing us to test our theoretical methods on a larger data range. For example, in data on the enhancement in the $e^+e^- \to \Lambda_c^+\Lambda_c^-$ cross sections reported by the Belle Collaboration [4], we could observe clearly two new charmonium resonances, viz. the $\psi(5S)$ and $\psi(4D)$ [5], as well as glimpses of what we believe to be the $\psi(6S)$ and $\psi(5D)$ [32] states. Furthermore, in data on $e^+e^- \to J/\psi\pi\pi$ and the $X(4260)$ enhancement published by the *BABAR* Collaboration [6, 7], we observed the $\psi(3D)$ resonance [8]. Finally, we identified an interference phenomenon between OZI-allowed and OZI-forbidden decay modes [9] near the $X(4260)$ enhancement in the *BABAR* data of Ref. [7].

It may have come as a surprise to our experimental colleagues that their observed enhancements could be interpreted either as normal $q\bar{q}$ resonances or as threshold effects, whereas sporadic coincidences with some of the countless states of the tetraquark, hybrid or molecular spectra, predicted by current theories and models of strong interactions, were not accompanied by a simultaneous description of the production data. If we compare this situation with the very good

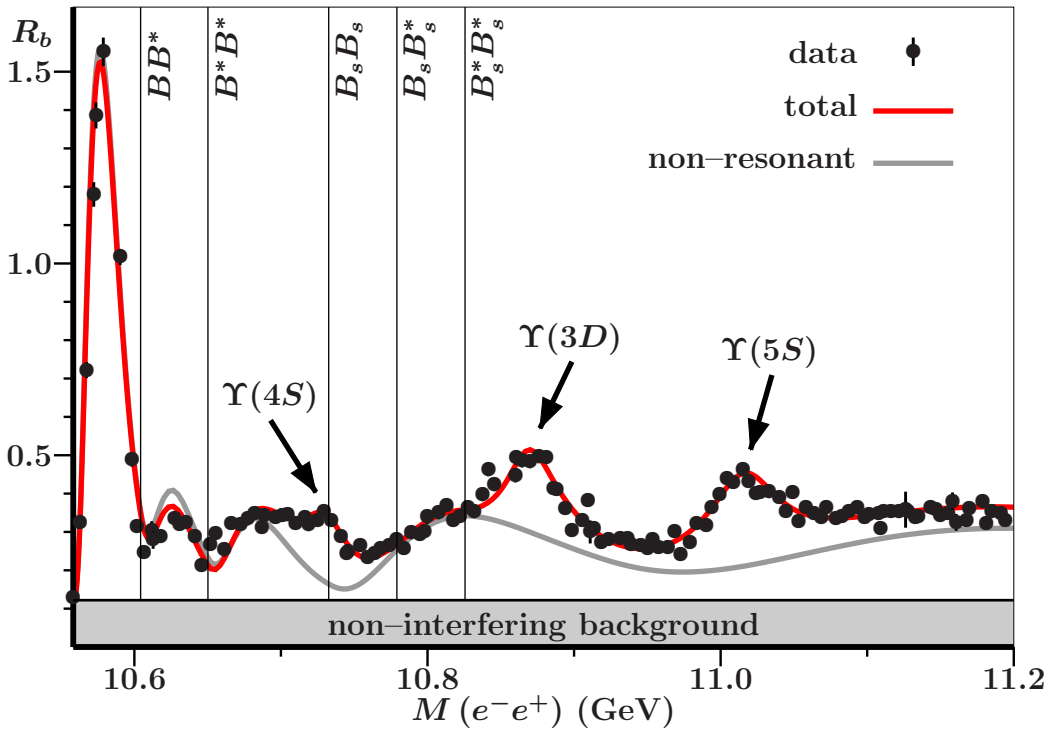

Figure 1: R_b as measured by *BABAR* [1] in electron-positron annihilation for energies between the $B\bar{B}$ and $\Lambda_b\bar{\Lambda}_b$ thresholds, vs. our model fit (—) as discussed in Secs. 2 and 3. The nonresonant contribution is also shown (—). Thresholds of $B\bar{B}^* + \bar{B}B^*$, $B^*\bar{B}^*$, $B_s\bar{B}_s$, $B_s\bar{B}_s^* + \bar{B}_sB_s^*$ and $B_s^*\bar{B}_s^*$ are indicated, as well as the central masses of the $\Upsilon(4S)$, $\Upsilon(3D)$ and $\Upsilon(5S)$ resonances.

description of experimental results for QED, it seems fair to conclude that strong interactions and, in particular, confinement are only poorly understood. Actually, we conclude that this is the real challenge from experiment to theory and models: to figure out what more is needed in

order to fully and in detail describe the experimental data, and not just the central masses of some bumps. In the present paper, we take up this challenge, hoping that it may contribute to a further understanding of the interactions between quarks and gluons, and their relation to the observed structures in scattering and production. Our results for vector bottomonium are depicted in Fig. 1 and will be discussed in Secs. 2 and 3.

From combined data, published by the *BABAR* Collaboration in Refs. [1,10], we concluded [5] that for the enhancement just above the $B\bar{B}$ threshold a description in terms of a wave function with a dominant $B\bar{B}$ component appears to be more adequate than assuming a pole in the scattering amplitude due to a supposed underlying $b\bar{b}$ state. Consequently, the enhancement does not represent the $\Upsilon(4S)$ resonance. We shall show that the true $\Upsilon(4S)$ lies about 160 MeV higher, viz. at 10.735 GeV.

In the following, we study data on hadron production in electron-positron annihilation in the invariant-mass interval between the $B\bar{B}$ and $\Lambda_b\bar{\Lambda}_b$ thresholds, published by the *BABAR* Collaboration [1]. This paper focuses on two of the resonances in the $b\bar{b}$ spectrum, using data obtained with the *BABAR* detector at the PEP-II storage ring, resulting in the Breit-Wigner (BW) parameters 10876 ± 2 MeV (mass) and 43 ± 4 MeV (width) for the $\Upsilon(10860)$, and 10996 ± 2 MeV (mass) and 37 ± 3 MeV (width) for the $\Upsilon(11020)$. These values differ substantially, in particular for the widths, from earlier results of the CUSB [11] and CLEO [12] Collaborations, and also from the world averages [13] 10865 ± 8 MeV (mass) and 110 ± 13 MeV (width) for the $\Upsilon(10860)$, and 11019 ± 8 MeV (mass) and 79 ± 16 MeV (width) for the $\Upsilon(11020)$. Obviously, such discrepancies call for further study.

In the present work, we apply a recently developed formalism for the study of hadronic electron-positron annihilation reactions to determine cross sections for open-bottom production above the $B\bar{B}$ threshold. The formalism is outlined in Sec. 2 and further discussed in Sec. 3. Details of the results are presented in Sec. 4. In Sec. 5 we propose future analyses on existing data in order to further clarify some of our findings. Conclusions are drawn in Sec. 6.

2 Open-bottom production in e^-e^+ annihilation

In Ref. [14], we derived a relation between the production amplitude $a_\ell(\alpha \to i)$ for e^+e^- annihilation into two mesons and the matrix elements of the meson-meson scattering amplitude T, resulting for the ℓ-th partial wave in an expression of the form

$$a_\ell(\alpha \to i) \propto g_{\alpha i}\, j_\ell\,(p_i r_0) + \frac{i}{2} \sum_\nu h_\ell^{(1)}\,(p_\nu r_0)\; g_{\alpha\nu}\, T_\ell(\nu \to i) \quad , \tag{1}$$

where the $g_{\alpha i}$ stand for the relative couplings of each of the two-meson systems i to a $q\bar{q}$ state of flavor α, and j_ℓ and $h_\ell^{(1)}$ are the spherical Bessel and Hankel function of the first kind, respectively. The radius r_0 represents the average distance at which the meson pair emerges from the interaction region. Furthermore, $\vec{p}_i$ is the relative linear momentum in two-meson channel i. The matrix element $T_\ell(\nu \to i)$ of the scattering amplitude T describes transitions between channels ν and i in multichannel meson-meson scattering.

The generic form of the scattering amplitude is, in the Resonance-Spectrum Expansion (RSE) [15], given by (with $M = \sqrt{s}$)

$$T_{ij}(M) = \frac{A_{ij}(M)}{D(M)} \quad , \tag{2}$$

which satisfies the unitarity condition

$$\Im m(D^* A_{ij}) = \sum_{\nu} A_{i\nu} A_{j\nu} \quad . \tag{3}$$

We have shown in Ref. [14] that relation (1) satisfies the extended unitarity theorem of Watson [16]. The denominator D of expression (2) is in the RSE given by the expansion

$$D(M) = 1 + 2i \sum_{n,\nu} \frac{g_{n\nu}^2 \, G_\nu(M)}{M - E_n} \quad . \tag{4}$$

The sum in Eq. (4) runs over the whole confinement spectrum ($n = 0, \ldots, \infty$), with levels given by E_n, and over all meson-meson channels involved, labeled by ν, the kinematics of which is contained in the functions $G_\nu(M)$. The relative couplings of the two-meson channels to the states of the confinement spectrum are given by $g_{n\nu}$ [17]. In Ref. [18], we showed that a denominator of the form given in Eq. (4) is equivalent to an effective meson theory with an infinite number of seeds, albeit with a well-defined mass spectrum.

The poles of the scattering amplitude can be searched for by solving the equation $D(M) = 0$ for complex values (or real ones when below the lowest threshold) of M. We have shown on several occasions in the past that D contains two types of poles, which can be distinguished by introducing an overall coupling λ, and letting the couplings $\lambda g_{n,\nu}$ continuously approach zero. Under this procedure we observe:

1. Poles that end up at the mass levels of the confinement spectrum [19, 20].

2. Poles that disappear in the lower half of the complex plane, with the imaginary part of the pole position [21] approaching minus infinity.

The behavior of the type-1 poles is exactly as expected for the RSE. Namely, when the system only couples weakly to the meson-meson sector, one expects narrow widths and small real mass shifts with respect to the underlying spectrum, like in photon absorption by hydrogen. Hence, for small coupling there are poles near each of the mass levels of the confinement spectrum, which, upon further decreasing the model's overall coupling, move towards these levels. For increasing overall coupling, these poles move further into the lower half of the complex invariant-mass plane, so as to end up at the positions where they are observed as resonances in experiment.

The type-2 poles are nowadays called *dynamically generated poles*, since they stem from the effective meson-meson interactions, which in the RSE are automatically contained in the denominator D. They do not have a simple relation to the confinement spectrum, which does not anticipate their existence. However, since the complete sum of all s-channel diagrams is equivalent to the sum of all t- and u-channel diagrams, by duality [22, 23], it is not a real surprise that upon summing up a certain class of strongly correlated s-channel exchanges [2, 3, 15], one effectively also accounts for part of the t-channel exchanges. Consequently, expression (2) contains both contributions, viz. the infinity of quark-antiquark resonances as well as the dynamically generated ones. This way we can easily generate additional scalar meson nonets, besides the ones stemming from the quark-antiquark spectrum, with the same set of parameters that fit the charmonium and bottomonium bound states and resonances. [21, 24].

In Ref. [25], the authors of the *Quarkonium Working Group* (QWG) contended that little work has been done concerning coupled-channel effects on quarkonium spectra since the original Cornell model [26, 27]. However, they must have overlooked a significant part of the literature

on the subject, as a lot of work has been done over the past 30 years on the important subject of relating scattering and production data to models for quarkonia spectra. In particular, a nonperturbative expression for the scattering amplitude, with the correct analyticity properties and moreover containing in a natural way the quarkonium spectrum, has been developed [2,3,15], thus enabling us to go beyond perturbative calculations [28], which may be unreliable for medium to large couplings. Furthermore, in Ref. [14] an amplitude for production was derived that allows for the comparison of quarkonium models with modern data of experimental hadronic physics. Heavy and light quarkonia are explained within the same formalism [3,21], with no need to resort to tetraquarks, meson molecules, or gluonic excitations [24]. Apparent difficulties for other quark models are no obstacles in the RSE, but have a common and quite natural explanation, like the mass of the $D_{s0}(2317)$ [29], and the masses of the $D_{s1}(2536)$ and $D_{s1}^*(2463)$ mesons [30]. The RSE predicted the shape of the $D_{sJ}(2860)$ production cross section [31], and even reasonably well the masses [2] of the tentative new [32] charmonium states $\psi(3D)$, $\psi(5S)$, $\psi(4D)$, $\psi(6S)$, and $\psi(5D)$. Other authors have made significant contributions to unitarization and coupled-channel effects as well, also ignored by the QWG [25]. It lies outside the scope of the present analysis to review all these results. Suffice it to mention the coupled-channel analysis of the $D_{s0}^*(2317)$ by Hwang and Kim [33], who computed the mass shift of the $1\,^3P_0$ $c\bar{s}$ state in the Cornell model, but also including the Coulombic part of the confining potential in the calculation of the transition amplitude between the $c\bar{s}$ and the two-meson sector, in contrast with the common practice to simply neglect this piece [26–28]. As a result, they found a mass shift that is a factor 2.6 larger than what would result from the standard Cornell procedure, thus allowing to obtain agreement with experiment. One can only speculate about the consequences for the Cornell predictions concerning charmonium and especially bottomonium, which are more compact systems than $c\bar{s}$ mesons, so that the importance of the Coulombic part of the potential is amplified.

In view of all these results, we are confident that, with some more effort, most meson-meson scattering and production amplitudes can be reproduced within the RSE [18]. Nevertheless, in the present paper we follow a different and more cumbersome path, in approximating expression (1) by a sum of BW resonances. This has the advantage of a more direct contact with experimental methods for extracting resonance poles from production cross sections. But more importantly, it gives us the opportunity to find out what extra ingredients, besides those already included in the RSE, are necessary for a full description of scattering and production data. Note, however, that bound states below the lowest threshold as well as the identification of dynamically generated resonances are lost in this procedure. Anyhow, before proceeding, we must first discuss the coupling of open-bottom pairs to $b\bar{b}$ states.

2.1 Coupling of open-bottom pairs to $b\bar{b}$

In the form presented in Eq. (1), the production amplitude consists of a nonresonant term, given by a Bessel function, and a sum of terms proportional to matrix elements of the scattering amplitude. Resonances reside in the latter matrix elements. Consequently, we have a clear separation of nonresonant and resonant terms for the production amplitude. We shall demonstrate in the following that such a separation is useful.

Expression (1), which was derived in the framework of the RSE [15], is a direct link between quark dynamics and quantities observed in experiment. However, in its present form the RSE scattering amplitude does not yet fully correspond to the physical reality, since it does not account very well for the experimental observation [34] that two-meson channels only couple significantly to the quark-antiquark propagator in a very limited range of energies close to threshold. From

harmonic-oscillator (HO) confinement, it is reasonably understood why a specific channel does not survive at higher invariant masses. Namely, it is straightforward to derive [17, 35] that the number of different channels to which the $q\bar{q}$ system couples grows rapidly for higher excitations. So for a given probability of quark-pair creation, the fraction that is left for a specific channel decreases accordingly.

All terms of the production amplitude of Eq. (1) are proportional to three-meson couplings, given by $g_{\alpha\nu}$. However, the three-meson couplings also enter the scattering amplitude T itself [14], that is, their squares. So at higher energies the terms containing the resonances fall off faster than the nonresonant term, leading to $q\bar{q}$ resonance peaks that fade away against background fluctuations of the nonresonant contribution in production cross sections. In Refs. [8, 32], we showed that signs of the $\psi(5S)$ and $\psi(4D)$ charmonium resonances can be observed just above threshold in the $e^+e^- \to \Lambda_c^+\Lambda_c^-$ cross section measured by the Belle Collaboration [4], with tentative $\psi(6S)$ and $\psi(5D)$ signals, at about 400 MeV higher invariant masses, almost drowned in the background.

Relative couplings are reasonably well determined by the formalism of Refs. [17,35]. However, as we mentioned above, the results of the experimental observation obtained with the SLAC/LBL magnetic detector at SPEAR [34] suggest that at higher invariant masses couplings vanish more rapidly than as follows from the RSE. The rate at which the couplings decrease still remains to be fully understood.

By the use of Eq. (1) and the three-meson couplings of Refs. [17,35], we may thus understand why it is hard to observe $q\bar{q}$ resonance peaks in scattering and especially production. However, from Ref. [34] we conclude that such a suppression may even be considerably larger, ranging from a factor 49 ± 25, determined via the process $\sigma\left(DD^*\right)/\sigma\left(D^*D^*\right)$, to a factor 124 ± 100, obtained from $\sigma\left(DD\right)/\sigma\left(D^*D^*\right)$, thereby already accounting for the combinatorial factors $PP : PV : VV = 1 : 4 : 7$ and scaling invariant mass with the RSE HO frequency ω. Consequently, we must take one step back in order to figure out what extra ingredient is needed to comply with the experimental evidence. Here, we focus on two-meson production reactions in e^+e^- annihilation, which we assume to take place via the coupling of the $q\bar{q}$ propagator to the photon.

In Refs. [17, 35], a relation between intermesonic distances and the strength of the three-meson coupling for configuration space was derived, assuming HO confinement and $^3P_0$ quark-pair creation. However, since for HO distributions Fourier transforms are obtained by the simple substitution of coordinate x by linear momentum k, one readily gets the corresponding relation between the three-meson coupling and relative linear momentum. In Fig. 2, we depict the shape of the three-meson vertex intensity [17] for the cases to be considered here. In the same figure, we show that this shape, being an approximation itself, can be further approximated quite well by a Gaussian shape [36].

For e^-e^+ annihilation into hadrons in the bottomonium region of invariant masses, we start out with the hypothesis that such processes take place through the $b\bar{b}$ propagator, and, moreover, that the amplitudes are dominated by loops of open-bottom mesons. The latter assumption implies that, even if the final state contains charmless hadrons, the line shape of its production cross section is to a large extent proportional to the line shape of open-charm production.

3 The BW expansion and its parameters

For each of the open-bottom final states one has an amplitude of the form given in Eq. (1). The total amplitude can be represented by a column vector. Each component of this vector

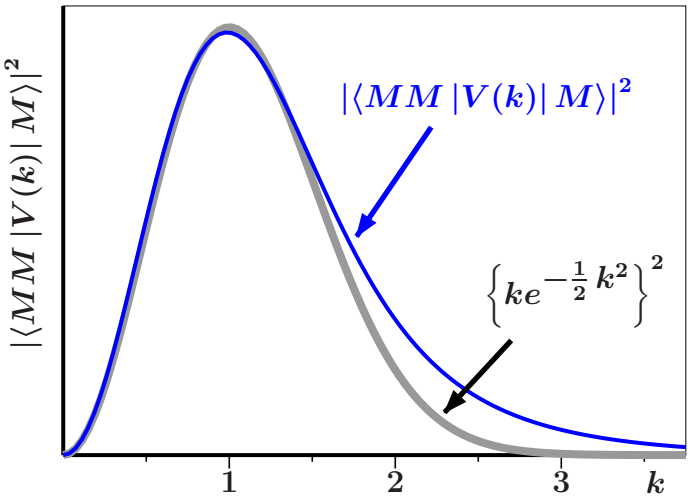

Figure 2: The shape of the three-meson vertex strength $\langle MM\,|V(k)|\,M\rangle$ as a function of the relative meson-meson linear momentum k (—), for $V \to PP$, $V \to PV$ and $V \to VV$ (V = vector, P = pseudoscalar) transitions [17], assuming HO confinement and $^3P_0$ quark-pair creation, and its approximation by a Gaussian shape (—). The matrix element $\langle MM\,|V(k)|\,M\rangle$ and the linear-momentum variable k, are dimensionless here.

contains the amplitude for decay into a specific channel. The intensity of the signal measured in experiment for one of the channels is proportional to the square of the modulus of the component which describes the transition of $b\bar{b}$ to that channel, e.g.

$$\sigma_\ell\left(b\bar{b} \to B\bar{B}\right) \propto \left|a_\ell\left(b\bar{b} \to B\bar{B}\right)\right|^2$$

$$\propto \left| g_{b\bar{b}\to B\bar{B}}\, j_\ell\left(p_{B\bar{B}} r_{0,\,B\bar{B}}\right) + \frac{i}{2}\sum_\nu h_\ell^{(1)}\left(p_\nu r_{0,\,\nu}\right)\, g_{\alpha\nu}\, T_\ell(\nu \to B\bar{B}) \right|^2 \quad , \tag{5}$$

where we allow r_0 to be different for each channel. The latter ingredient is a generalization of Eq. (1), But it is useful, as we shall see furtheron.

Each of the scattering amplitudes $T_\ell(\nu \to B\bar{B})$ has the form as given in Eq. (2), which implies that the pole structure, given by the zeros of expression (4), is the same for all of them. As a consequence, the full sum on the righthand side of Eq. (5) has a structure of the form shown in Eq. (2). Hence, we may approximate this full sum by a sum of BW expressions, according to

$$\frac{i}{2}\sum_\nu h_\ell^{(1)}\left(p_\nu r_{0,\,\nu}\right)\, g_{\alpha\nu}\, T_\ell(\nu \to B\bar{B}) \to g_{b\bar{b}\to B\bar{B}} \sum_R b_{R,\,B\bar{B}}\, e^{i\varphi_{R,\,B\bar{B}}}\, A_R\,(\mathrm{BW}) \quad , \tag{6}$$

where R runs over all poles in the scattering amplitude, which are, in principle, infinite in number. In practice we limit us, of course, to the number of likely candidates in the invariant-mass interval under consideration. Notice that we have suppressed the relative angular-momentum quantum number ℓ.

The expansion coefficients that show up in the sum on the righthand side of Eq. (6) are complex numbers. We have separated the moduli b_R and the phases φ_R of these coefficients, similarly to what is common practice in experimental analysis. The BW amplitudes are given by

$$A_R\,(\mathrm{BW})\,(\sqrt{s}) = \frac{\omega}{M_R - 2m_B}\,\frac{\Gamma_R/2}{\sqrt{s} - M_R + i\Gamma_R/2} \quad , \tag{7}$$

where $\sqrt{s}$ and $M_R - i\Gamma_R/2$ are the total invariant mass and the pole position of resonance R in the complex E plane, respectively. Since the positions of the poles in the complex invariant-mass plane are, moreover, the same for all channels, the BW amplitudes are independent of the channel index. Furthermore, by the use of Eq. (4), one may deduce that the BW expansion for the RSE is linear in the masses, and not quadratic as in the so-called *relativistic* expressions. As a consequence, we may find small deviations from the findings of the *BABAR* Collaboration for the resonance pole positions. The factor $\omega/\left(M_R - 2m_B\right)$ is inserted to account for the invariant-mass dependence of the $b\bar{b}$ propagator, which is supposed to be the principal origin of resonances.

For Eq. (5) we then get the approximation

$$\sigma_\ell\left(b\bar{b} \to B\bar{B}\right) \propto \left| g_{b\bar{b}\to B\bar{B}}\, j_\ell\left(p_{B\bar{B}} r_{0,\,B\bar{B}}\right) + \sum_R b_{R,\,B\bar{B}}\, e^{i\varphi_{R,\,B\bar{B}}}\, A_R\left(\mathrm{BW}\right) \right|^2 \quad . \tag{8}$$

At this point we insert the form factor indicated in Fig. 2 for the coupling of $b\bar{b}$ to $B\bar{B}$, thereby also introducing some overall constant λ. Thus, we obtain the final expression

$$\sigma_\ell\left(b\bar{b} \to B\bar{B}\right) = \tag{9}$$

$$= \lambda_{B\bar{B}}^2\, p_{B\bar{B}}^2 r_{0,\,B\bar{B}}^2\, e^{-p_{B\bar{B}}^2 r_{0,\,B\bar{B}}^2} \left| g_{b\bar{b}\to B\bar{B}}\, j_\ell\left(p_{B\bar{B}} r_{0,\,B\bar{B}}\right) + \sum_R b_{R,\,B\bar{B}}\, e^{i\varphi_{R,\,B\bar{B}}}\, A_R\left(\mathrm{BW}\right) \right|^2 .$$

The here to be analyzed experimental data for R_b, published by the *BABAR* Collaboration [1], contain final states of various different open-beauty channels. We assume that such a signal is proportional to the sum of the individual cross sections, by summing them up incoherently, according to

$$R_b \propto \frac{3s}{4\pi\alpha^2} \left\{ \sigma_\ell\left(b\bar{b} \to B\bar{B}\right) + \sigma_\ell\left(b\bar{b} \to B\bar{B}^*\right) + \ldots \right\} \quad . \tag{10}$$

Note that this expression has enough parameters to fit a herd of elephants [37]. In the following, we shall discuss these parameters and try to establish some order among them.

In order to account for channels that open at energies above the $B_s^*\bar{B}_s^*$ threshold, we introduce a hypothetical seventh channel, called BX, with threshold at $m_B + m_X$, where m_X remains a free parameter. As a result of our analysis below, we find for the mass of the open-bottom X meson an optimum value of 5.634 GeV. This looks very reasonable in view of the observation of further B-type mesons at energies above 5.72 GeV, and widths varying from a few tens of MeV to 130 MeV. We assume here that the BX channel is in a P wave, although different quantum numbers are certainly possible. Our BX channel should effectively substitute all possible channels in the invariant-mass region from about 10.9 GeV upwards. Its threshold turns out to lie a little bit lower than the mentioned value of 5.72 GeV, which may account, also in an effective sense, for the hadronic widths of the open-bottom mesons heavier than the B_s^*.

3.1 The 21 phases of the Υ resonances

Each of the three resonances considered in this work has a phase difference with respect to the nonresonant amplitudes of each of the seven channels involved in our analysis. So this implies 21 phases in total. If taken as parameters freely adjustable to the data, this is a sufficiently [38] large number to fit a little elephant [39]. Fortunately, it is easy to understand what these phases originate from and therefore how to restrict their arbitrariness.

The bare states of the $b\bar{b}$ spectrum have a level spacing of 2ω in the HO approximation to the RSE (HORSE [40]). Except for the ground state, we find two $J^{PC} = 1^{--}$ states at each level: one for which the bottom quarks are in a relative S wave, and one in a D wave. Hence, we expect phases to jump by an amount of 2π over a mass difference of 2ω. This suggests π/ω as the scale for phase differences.

The phase at the mass of resonance R in two-meson channel A must be related to the mass difference between the channel's threshold $m_{A1} + m_{A2}$ (m_{A1} and m_{A2} are the meson masses) and the central resonance position M_R. If we moreover assume the relation to be linear to lowest order, then we obtain something of the form

$$\varphi(R, A) = \varphi_R + \frac{m_{A1} + m_{A2} - M_R}{\omega}\,\pi \quad , \tag{11}$$

where the 3 values for φ_R would in principle remain as free parameters. Nevertheless, also these values can be determined, as we shall explain below.

The central mass positions of resonances do not appear at the levels of the HO in the HORSE. Meson loops shift these masses to their physical values. A comparable situation concerning electromagnetic interactions exists for the level spectrum of atoms and molecules. For example, the mass spectrum of the hydrogen atom H can be made visible through electromagnetic interactions. It appears in the spectrum of $\gamma + H \to \gamma + H$ in the form of narrow absorption lines. However, as one learns in atomic-physics courses, the invariant masses of such lines do not correspond to the exact mass values of the bare hydrogen levels. They appear at slightly shifted masses and, moreover, with a certain line width, both of which can be calculated using perturbative methods. In the case of strong interactions, perturbative theory is of little use, whatever beautifull Lagrangians may serve as a starting point. Nevertheless, one must count with sizable mass shifts and line widths, which are indeed observed in experiment. Here, we assume the existence of a bare $b\bar{b}$ spectrum $E_{n\ell}$ (n for radial and ℓ for angular excitations) given by the HORSE, reading [2, 18]

$$E_{n\ell} = 2m_b + \omega\left(2n + \ell + \tfrac{3}{2}\right) \quad . \tag{12}$$

The mass shifts and line widths are determined in the RSE nonperturbatively.

The referred mass shifts cause further phases, which are opposite in sign. Now, in general, one does not know very much about the levels of the bare states. But in the HORSE they can be determined by using the parameters optimized and fixed in Ref. [3]. For the reference mass we can take any of the states of the $J^{PC} = 1^{--}$ HO spectrum, since, in the linear approximation, their phases differ by steps of exactly 2π. We shall choose here the $3D$ bare-state mass $M_{\rm bare}(3D)$, because it comes out around the mass center of the resonances to be analyzed. With the values $\omega = 0.190$ GeV and $m_b = 4.724$ GeV [3], and also using Eq. (12), we find

$$M_{\rm bare}(3D) = 2\,m_b + \frac{15}{2}\,\omega = 10.873 \ \ {\rm GeV} \quad , \tag{13}$$

while for φ_R we obtain

$$\varphi_R = \frac{M_{\rm bare}(3D) - M_R}{\omega}\,\pi \quad . \tag{14}$$

Consequently, all 21 phases can be determined, without any freedom, by the use of the values of two well-established parameters for the HORSE.

So how about fitting then the little elephant [1] of *BABAR*? Well, the reader should not worry, there are still plently of parameters left so far.

3.2 The 21 moduli of the Υ resonances

Each of the three resonances R considered in this work couples to each of the seven channels A involved in our analysis. So this implies 21 moduli $b_{R,A}$ in total. However, if we carefully study the expressions in Eqs. (5,6), we observe that the BW expansion stems from a weighted sum over elastic and inelastic matrix elements of the scattering amplitude. To leading order, we may assume that the elastic matrix element dominates the expression. As a consequence, $b_{R,A}$ is, to leading order, proportional to $g_{R,A}$, which allows us to interrelate the moduli, since the couplings of bare states to the open-bottom meson-meson channels just involve combinatorial factors. Explicitly, writing $B\bar{B}$ for $\left|b_{R,B\bar{B}}\right|^2$ and similarly for the other channels, one has for the considered cases

$$B\bar{B} \,:\, BB^* \,:\, B^*\bar{B}^* \,:\, B_s\bar{B}_s \,:\, B_sB_s^* \,:\, B_s^*\bar{B}_s^* \,=\, 2 \,:\, 8 \,:\, 14 \,:\, 1 \,:\, 4 \,:\, 7 \quad . \tag{15}$$

This way, we may limit the number of free parameters to the moduli $b_{R,B\bar{B}}$ of the three resonances to the $B\bar{B}$ channel. All the others can be determined via the combinatorial factors of Eq. (15). The seventh channel, viz. $B + X$, is treated separately. Since we assume this channel to be in a P wave, we may estimate its branching fraction by inspecting all possible P-wave channels with one B meson plus something else. We find that the total intensity of such channels is twice as large as the intensity for $B\bar{B}$. Thus, we use for $B + X$ a combinatorial factor $\sqrt{2}$.

Furthermore, in the HORSE we may also determine the relative intensities for $4S$, $3D$ and $5S$ to $B\bar{B}$ [17, 35], obtaining

$$b(4S, B\bar{B}) \,:\, b(3D, B\bar{B}) \,:\, b(5S, B\bar{B}) \,=\, 1 \,:\, \frac{2}{\sqrt{3}} \,:\, \frac{\sqrt{11}}{6} \quad . \tag{16}$$

Consequently, we are left with one free parameter only, namely $b(4S, B\bar{B})$, for the 21 moduli pertaining to the three Υ resonances. Moreover, the mere fact that the combinatorial factors of Eq. (16) lead to a correct description of the data, as one may observe in Fig. 1, lends further support to the assignments proposed in this paper for the three resonances at 10.735, 10.867, and 11.017 GeV.

3.3 The 7 couplings of the meson-meson channels to $b\bar{b}$

What is so special about the $b\bar{b}$ case that cannot be observed equally clearly for $c\bar{c}$, and even less so in the light quark sector, is the fact that the lightest thresholds are separated in one set for open bottom accompanied by light quarks, viz. $(b\bar{u})(u\bar{b})$ and $(b\bar{d})(d\bar{b})$, and another set for open bottom with strange quarks: $(b\bar{s})(s\bar{b})$. This very special situation opens a window for a detailed study of the production of quarks and antiquarks in electron-positron annihilation.

In the HORSE, the $B\bar{B}$ threshold at 10.56 GeV lies far above the HO ground state at 9.72 GeV and the first radial excitation at 10.10 GeV, and also above the second radial excitation at 10.48 GeV. Note that the radial level spacings are equal to $2\omega = 0.38$ GeV in the HORSE. The three-meson vertex intensities for these HO levels can be determined with the formalism developed in Ref. [17]. The total $B\bar{B}$ branching fraction is found to be roughly 2.8% at the HO ground state, but only about 0.4% at the second radial HO excitation. The main competition for $B\bar{B}$ formation above the $B\bar{B}$ threshold stems from the BB^* channel. This competing channel will start to dominate for invariant masses closer to the BB^* threshold at 10.60 GeV. Above the BB^* threshold, we suppose that $B\bar{B}$ formation rapidly vanishes.

The above implies that at the BB^* threshold the coupling of $B\bar{B}$ to the $b\bar{b}$ propagator must have decreased significantly. This is indeed confirmed by Fig. 3, in which we show data for the process $e^+e^- \to b\bar{b}$, measured and analysed by the *BABAR* Collaboration [1]. As also remarked in their paper, the large statistics and the small energy steps of the scan make it possible to clearly observe the two dips at the opening of the thresholds corresponding to the $B\bar{B}^* + \bar{B}B^*$ and $B^*\bar{B}^*$ channels. We have cut off the huge peak at 10.58 GeV, in order to concentrate better on the details of the other two enhancements, at 10.63 GeV and 10.69 GeV, respectively. Near the BB^* threshold, we thus observe that the $B\bar{B}$ signal rapidly vanishes for increasing invariant mass, whereas the BB^* signal behaves the opposite way, i.e., it grows fast for increasing invariant mass just above threshold. At the B^*B^* threshold, this phenomenon is repeated, now with respect to the BB^* signal.

So we conclude that $B\bar{B}$ production in e^+e^- annihilation can mainly be observed within the invariant-mass window delimited by the $B\bar{B}$ and BB^* thresholds. Similarly, BB^* production has an equally wide window formed by the BB^* and B^*B^* thresholds. The window for B^*B^* production is somewhat wider, since the next threshold concerns the B_sB_s channel, which lies considerably higher. Therefore, the enhancement peaking at about 10.69 GeV is broader than the ones at 10.58 and 10.63 GeV.

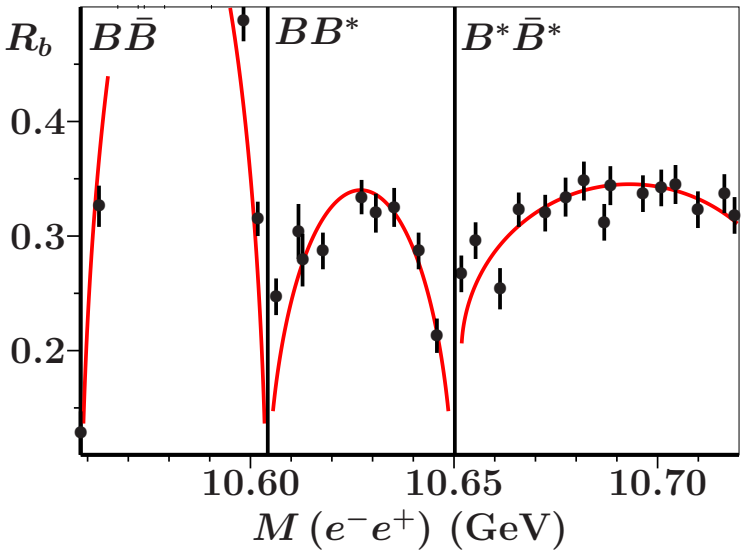

Figure 3: Experimental data for the process $e^+e^- \to b\bar{b}$ measured by the *BABAR* Collaboration [1]. The vertical lines indicate the BB^* and B^*B^* thresholds, as indicated in the figure. The eye-guiding lines reflect our interpretation of the data, and do not represent fits.

The above observations must somehow be contained in the coupling constants $g_{b\bar{b}\to B\bar{B}}$, $g_{b\bar{b}\to BB^*}$, and $g_{b\bar{b}\to B^*\bar{B}^*}$ (see Eq. (9)), since these quantities regulate the intensity of the nonresonant contribution to the total production amplitude. Indeed, after taking out the combinatorial factors as given in Eq. (15), and by defining

$$g_{b\bar{b}\to B\bar{B}} = 2g\left(B\bar{B}\right) \quad , \quad g_{b\bar{b}\to BB^*} = 8g\left(BB^*\right) \quad , \quad g_{b\bar{b}\to B^*\bar{B}^*} = 14g\left(B^*\bar{B}^*\right) \quad , \tag{17}$$

we find that the 3 residual couplings $g\left(B\bar{B}\right)$, $g\left(BB^*\right)$, and $g\left(B^*\bar{B}^*\right)$ are not equal, as one would naively expect, but that there remains a strong dependence on invariant mass. In the left part of Fig. 4, we show the values of these 3 residual couplings, normalized to $g\left(B\bar{B}\right)$. Following

an analogous procedure, also using the combinatorial factors given in Eq. (15), we determine the remaining 3 residual couplings for the sector where $s\bar{s}$ quark-pair creation is supposed to lead to bottom-strange meson pairs. The latter ones are shown in the right part of Fig. 4. Moreover, the values for the couplings in the $(b\bar{s})(s\bar{b})$ sector are multiplied by a factor 4, in order to better notice the common behavior of the couplings to PP, PV, and VV (V = vector, P = pseudoscalar). In each sector, we have depicted 3 curves. They are scaled with the size of the window, namely $m\,(B^*) - m\,(B)$, in the bottom-light sector, and $m\,(B_s^*) - m\,(B_s)$ in the bottom-strange sector. We assume that our coupling "constants" are actually a kind of average values for the intensity of open-bottom pair production in electron-positron annihilation, that is, averaged over the relevant interval. Hence, the curves shown in Fig. 4 represent the picture we imagine for the actual dependence of these intensities on invariant mass.

We conclude from the results of Fig. 4 that apparently two different processes are responsible for the production of pairs of open-bottom mesons in electron-positron annihilation, namely one according to the reaction

$$e^- e^+ \to n\bar{n} \to (n\bar{b})(b\bar{n}) \quad , \tag{18}$$

for n representing either up or down quarks, and the other through the reaction

$$e^- e^+ \to b\bar{b} \to (b\bar{n})(n\bar{b}) \quad , \tag{19}$$

with an analogous situation in the $(b\bar{s})(s\bar{b})$ sector, upon substituting n by s. At higher invariant

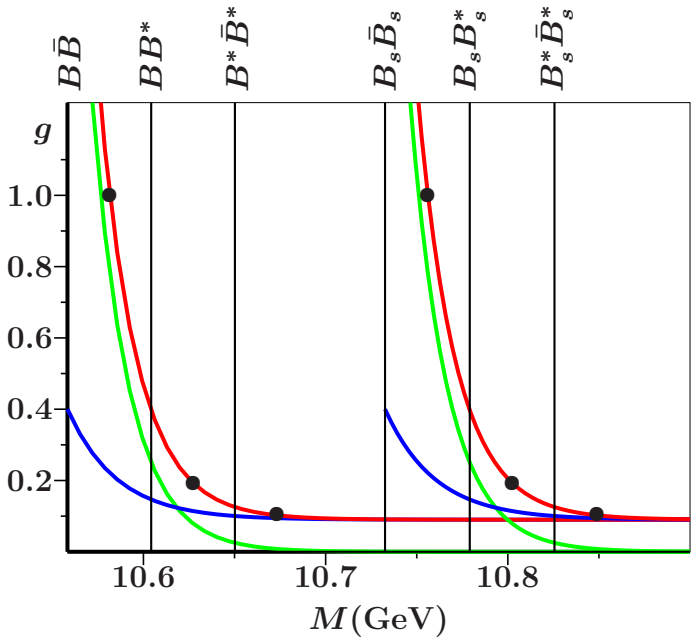

Figure 4: Values of the various parameters g (•) used in this work. From left to right: $g\left(B\bar{B}\right)$, $g\left(B\bar{B}^*\right)$, $g\left(B^*\bar{B}^*\right)$, $g\left(B_s\bar{B}_s\right)$, $g\left(B_s\bar{B}_s^*\right)$, and $g\left(B_s^*\bar{B}_s^*\right)$. The values are given in the centers of the corresponding invariant-mass intervals. The couplings in the $(b\bar{s})(s\bar{b})$ sector have been multiplied by a factor 4. The vertical lines indicate the respective thresholds (see also Fig. 1). See the text for an explanation of the curves.

masses, the reaction (19) and its equivalent upon substitution of n by s seem to dominate the production of pairs of open-bottom mesons, whereas near the $B\bar{B}$ and $B_s\bar{B}_s$ thresholds the

reaction (18) and its $n \to s$ equivalent appear to be dominant. We have indicated the evolution of the couplings, as we imagine it, with respect to invariant mass of the former reactions by (—), and of the latter ones by (—). The curves (—) represents the sum of the couplings of the two distinct reactions.

At this stage, the reader may like to be informed on the margin of freedom for the various couplings. We have not performed a complete analysis of possible error bars on the values we used for the theoretical curve of Fig. 1. However, as far as we could deduce, the margin of freedom is small, possibly largest for $g\left(B_s^* \bar{B}_s^*\right)$. But even the latter margin does not exceed a few percent, at most 10%. Consequently, the error in the factor 4 for the couplings of the $(b\bar{s})(s\bar{b})$ sector with respect to the $(b\bar{n})(n\bar{b})$ sector does certainly not exceed 10% and is most probably just a few percent. In the present work we have fixed this factor at 4, which might stem from some underlying symmetry we are currently not aware of. For invariant masses larger than the upper limit of Fig. 4, we expect the residual couplings of the two sectors to be equal. This implies that the curve of the $(b\bar{n})(n\bar{b})$ sector must still decrease by a factor 4 with respect to the curve of the $(b\bar{s})(s\bar{b})$ sector. But this is not relevant for the present analysis. In total we are thus left with 4 free coupling parameters: the 3 couplings in the $(b\bar{n})(n\bar{b})$ sector and the coupling to the seventh channel, BX. The latter coupling, which represents several channels that open at higher invariant masses, cannot be related to the others. Here, we have used the value $g\left(BX\right)/g\left(B\bar{B}\right) = 0.150$ for the theoretical curve of Fig. 1.

Let us now come back to our interpretation of the results of Fig. 4. Near the $B\bar{B}$ and $B_s\bar{B}_s$ thresholds, we concluded that open-bottom pairs dominantly couple to an initial $n\bar{n}$ and $s\bar{s}$ pair, respectively. The subsequent $b\bar{b}$ creation then takes place via an OZI-allowed strong process. Only for higher invariant masses the primary creation of $b\bar{b}$ is the main source for open-bottom pairs via the ensuing OZI-allowed creation of a light quark pair. Therefore, we may conclude that so far we have bet on the wrong HORSE, by assuming that primary $b\bar{b}$ creation is the dominant process above (and below) the $B\bar{B}$ threshold.

As a consequence of these observations, we seem to may consider initial $b\bar{b}$ creation only to be dominant for higher invariant masses. This is possibly what also should be concluded from the data for the R ratio, where one does not observe a diminishing of the creation of lighter quark pairs, but just an additional pair creation of the heavier type of flavors. So it is not at all clear which of the two processes, viz. (18) or (19), will be dominant at which energy. Here, we conclude that the latter reaction for open-bottom meson-pair creation only starts dominating at higher invariant masses.

A discussion on the formation of open-bottom mesons is here in place. It has always been assumed that once enough energy is available, meson pairs can be created. However, in $p\bar{p}$ annihilation that is not what has been observed [41]. Although in this process enough energy is available for the creastion of pion pairs, Nature prefers to create larger numbers of pions, most probably via intermediate resonances. Hence, there seems to be a stability question at hand. We conclude from the above observation that a stable pair of $B\bar{B}$ mesons is more easily produced via an initial pair of b quarks (Eq. (19)), but that at low kinetic energies an initial pair of nonstrange quarks can also produce $B\bar{B}$ mesons. Light quark pairs are produced more abundantly, hence dominate near the $B\bar{B}$ threshold.

The fact that this phenomenon is repeated at the opening of the $B_s\bar{B}_s$ threshold lends further credit to our picture. It also rebuts the possible criticism that by taking a much larger value for $g_{b\bar{b}\to B\bar{B}}$ than for the other two couplings, $g_{b\bar{b}\to BB^*}$ and $g_{b\bar{b}\to B^*\bar{B}^*}$ we *generate* the enhancement at 10.58 GeV. Namely, it would be too much of a coincidence to observe exactly the same phenomenon in the $s\bar{s}$ sector. In the next section we shall find that the radii corroborate the

above picture.

3.4 The 7 values for r_0

The parameter r_0, which was introduced in Ref. [2] in order to allow for a quantity representing the average distance of quark-pair creation, requires renewed attention. In Fig. 5 we have depicted

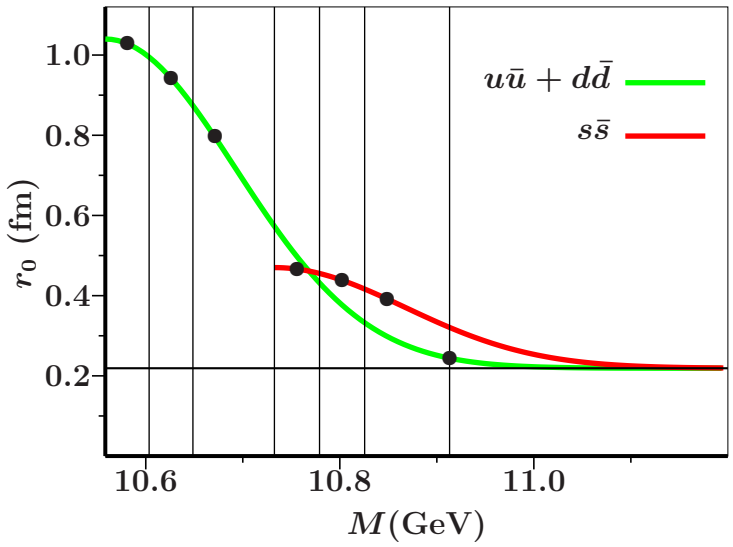

Figure 5: Values of the various parameters r_0 (•) used in this work. From left to right: $r_0\left(B\bar{B}\right)$, $r_0\left(B\bar{B}^*\right)$, $r_0\left(B^*\bar{B}^*\right)$, $r_0\left(B_s\bar{B}_s\right)$, $r_0\left(B_s\bar{B}_s^*\right)$, $r_0\left(B_s^*\bar{B}_s^*\right)$, and $r_0\left(BX\right)$. The values are given at the invariant masses where the respective channels open. The solid lines, viz. (—) for $n\bar{n}$ ($u\bar{u}$ or $d\bar{d}$) and (—) for $s\bar{s}$ pair creation, are given by Eqs. (20,21), for $r_{b\bar{b}} = 0.221$ fm, $r_{n\bar{n}} = 1.04$ fm and $r_{s\bar{s}} = 0.47$ fm. The vertical lines indicate the respective thresholds (see also Fig. 1).

the values for the various radii $r_0\left(B\bar{B}\right)$, $r_0\left(B\bar{B}^*\right)$, $r_0\left(B^*\bar{B}^*\right)$, $r_0\left(B_s\bar{B}_s\right)$, $r_0\left(B_s\bar{B}_s^*\right)$, $r_0\left(B_s^*\bar{B}_s^*\right)$, and $r_0\left(BX\right)$, which have been used for the theoretical curve of Fig. 1. Just above the $B\bar{B}$ threshold we find values of the order of 1 fm, corresponding to light quarks, as expected from the picture for $B\bar{B}$ creation, discussed in the preceding subsection. Similarly, we find values of about 0.45 fm just above the $B_s\bar{B}_s$ threshold, corresponding to a system of $s\bar{s}$ pairs.

For higher invariant masses the radii tend towards 0.221 fm, which corresponds to the size of systems of $b\bar{b}$ pairs. Hence, the findings for the radii seem to corroborate the picture that at low kinetic energies the reaction of Eq. (18) dominates, whereas at higher kinetic energies this reaction cannot provide the necessary stability for $B\bar{B}$ creation, so that the reaction of Eq. (19) is dominant.

Consequently, we have learned here that our previous approach to meson-meson production processes, where in the HORSE we only assumed the reaction of Eq. (18) to be relevant, is not in full agreement with the experimental observations. Apparently, near the lowest thresholds we must also consider processes that are dominated by the initial production of light quark pairs. This very valuable result of the present analysis should henceforth be incorporated in the HORSE. For the light quark sector it will not have any influence, since there is no difference in the reactions of Eqs. (18) and (19) when b is replaced by n. It may have some consequences for the description of $s\bar{s}$ systems, but for $c\bar{c}$ and, as we have seen here, for $b\bar{b}$, inclusion of the light-quark processes will certainly have some influence near the opening of the lowest lying open-charm and

open-bottom thresholds. However, for higher invariant masses the results of the HORSE will not change dramatically. In particular, the spectra for light and heavy quarkonia predicted by the HORSE will only change marginally, as we may conclude from the present analysis.

It is possible to parametrize the curves shown in Fig. 5, thus reducing the number of effective parameters. We have opted for the Gaussian expression

$$r_{n\bar{n}}(M) \;=\; r_{b\bar{b}} + \{r_{n\bar{n}} - r_{b\bar{b}}\}\; e^{-\left\{(M\,-\,2m_{B\,/\,B_s})/\omega\right\}^2} \quad , \tag{20}$$

and an analogous one with n replaced by s. For $r_0(B\bar{B})$ we have chosen the average value for $r_0(n\bar{n})$ in the window for $B\bar{B}$ production, viz. $\Delta(n\bar{n})$, which extends from the $B\bar{B}$ threshold to the BB^* threshold, i.e., $\Delta(n\bar{n}) = m_{B^*} - m_B$. To be more precise, we have just chosen

$$r_0(\left(\begin{array}{c} B\bar{B} \\ BB^* \\ B^*\bar{B}^* \end{array}\right)) = r_{n\bar{n}}(M = \left(\begin{array}{c} 2m_B \\ m_B + m_{B^*} \\ 2m_{B^*} \end{array}\right) + \tfrac{1}{2}\Delta(n\bar{n})). \tag{21}$$

In the $(b\bar{s})(s\bar{b})$ sector the procedure is analogous, but with the window for $B\bar{B}$ production replaced by that for $B_s\bar{B}_s$ production, that is, $\Delta(s\bar{s}) = m_{B_s^*} - m_{B_s}$. For the BX channel we have chosen the value of our parametrization at the BX threshold.

3.5 Compilation of the free parameters

We now absorb the factor $4\pi\alpha^2$ of the R_b ratio, given in Eq. (10), in the 5 free coupling constants $b_{\Upsilon(4S),B\bar{B}}$, $\lambda_{B\bar{B}}$, λ_{BB^*}, $\lambda_{B^*\bar{B}^*}$ and λ_{BX} of the 7 contributions. Our final expression is then given by

$$R_b = \frac{3s}{\omega^2}\,\left\{\sigma_\ell\left(b\bar{b} \to B\bar{B}\right) + \sigma_\ell\left(b\bar{b} \to BB^*\right) + \ldots\right\} \quad . \tag{22}$$

The resulting values for the couplings are collected in Table 1.

We do not include the HORSE frequency $\omega = 190$ MeV in the list of free parameters. It has been fixed in Ref. [3] by carefully studying the average mass splittings in the light and heavy quarkonia. In all our work over almost three decades, we have never changed ω, not even by as little as a tenth of an MeV. So ω is something similar to the pion decay constant in other models, though more stable over the course of time. Furthermore, $m_b = 4724$ MeV has also been taken from Ref. [3], and therefore is not considered a free parameter here.

The parameter r_b, which could have been determined from the parameters $\rho_0 = 0.56$ and $m_b = 4724$ in Ref. [3], yielding

$$r_b = \frac{\rho_0 \hbar c}{\sqrt{\omega m_b/2}} = 0.165 \;\; \text{fm} \quad , \tag{23}$$

optimizes here at $r_b = 0.22$ fm. This slightly larger value may be due to the different transition potentials for the $b\bar{b}$ states to the open-bottom meson-meson channels, as used for the results in Ref. [3] and for the formula in Eq. (1), respectively. Namely, in Ref. [3] a spatially extended potential was employed, peaking at a distance given by ρ_0 and the quark masses, whereas Eq. (1) results from a potential only acting at r_b. The corresponding delta shell does not necessarily come out at the same position as the peak of the spatially extended potential. Therefore, we have considered r_b a free parameter here.

Parameter(s)	Value(s)
non-interfering background	0.122
$b_{\Upsilon(4S),B\bar{B}}$	0.108
$\lambda_{B\bar{B},BB^*,B^*\bar{B}^*}$	2.28, 0.436, 0.236
m_X, λ_{BX}	5.634 GeV, 0.150
$r_{n\bar{n},s\bar{s},b\bar{b}}$	1.04 fm, 0.47 fm, 0.221 fm
$M_{\Upsilon(4S)}$, $\Gamma_{\Upsilon(4S)}$	10.735 GeV, 38 MeV
$M_{\Upsilon(3D)}$, $\Gamma_{\Upsilon(3D)}$	10.867 GeV, 42 MeV
$M_{\Upsilon(5S)}$, $\Gamma_{\Upsilon(5S)}$	11.017 GeV, 59 MeV

Table 1: Parameters used for the theoretical curve of Fig. 1.

In Sec. 3.1, we saw that the phases of the resonances are completely determined by the parameters ω and m_b of Ref. [3]. Hence, there are no free phases. Furthermore, in Sec. 3.2 we found that all moduli are given by one free parameter, viz. $b(4S, B\bar{B})$.

For the data of the *BABAR* Collaboration [1], which amount to the R_b ratio for all e^+e^- annihilation processes containing b quarks, we assume a background of $R_b = 0.122$, to account for those reactions that do not contain open-bottom pairs.

A possible criticism that 16 parameters are enough to fit whatever line shape would not be fair. In an experimental analysis of the here considered data set, one would use $3 \times 4 = 12$ BW parameters for the three resonances, at least one parametere for the non-interferening background, and another two parameters for a nonresonant background interfering with the resonances, thus totaling a minimum number of 15 parameters. However, such an analysis would certainly not be capable of describing the $B\bar{B}$ enhancement at 10.580 GeV. Were the latter structure also described by a BW, the experimental analysis would need as many as 19 paramenters. So it seems reasonable to conclude that our excellent description of the data in Fig. 1 is a good and reliable result.

4 Results

The higher excitations of the bottomonium vector states, discovered more than two decades ago, are still today a puzzling topic of intensive research. In Refs. [11] and [12], the CUSB and CLEO Collaborations, respectively, presented the first results for the invariant-mass spectra of the $R\,(\sigma_{\rm had}/\sigma_{\mu\mu})$ ratio above the open-bottom threshold.

The data of Ref. [11] were observed with the CUSB calorimetric detector operating at CESR (Cornell). The experimental analysis resulted in evidence for structures at 10577.4 ± 1 MeV, 10845 ± 20 MeV, and 11.02 ± 0.03 GeV, with total hadronic widths of 25 ± 2.5 MeV, 110 ± 15 MeV, and 90 ± 20 MeV, respectively. Structures at about 10.68 and 11.2 GeV were not included

in the analysis of the CUSB Collaboration.

The data of Ref. [12] were obtained from the CLEO magnetic detector, also operating at CESR. The experimental analysis resulted in evidence for structures at $10577.5 \pm 0.7 \pm 4$ MeV, $10684 \pm 10 \pm 8$ MeV, $10868 \pm 6 \pm 5$ MeV, and $11019 \pm 5 \pm 5$ MeV, with total hadronic widths of $20 \pm 2 \pm 4$ MeV, $131 \pm 27 \pm 23$ MeV, $112 \pm 17 \pm 23$ MeV, and $61 \pm 13 \pm 22$ MeV, respectively. A structure at about 11.2 GeV was not included in the analysis of the CLEO Collaboration.

In Tables 2, 3, 4 and 5 we compare our results for the three resonances $\Upsilon(4S)$, $\Upsilon(3D)$ and $\Upsilon(5S)$ to the values published more than two decades ago by the CUSB [11] and CLEO [12] Collaborations, as well as to the more recent data of the *BABAR* Collaboration [1] and the world averages given by the Particle Data Group in Ref. [13].

4.1 The $B\bar{B}$ enhancement at 10.580 GeV

The enhancement at 10.580 GeV was extensively studied in a more recent publication [10] of the *BABAR* Collaboration. Data were collected with the *BABAR* detector at the PEP-II storage ring of Stanford Linear Accellerator Center. The experimental analysis yielded $10579.3 \pm 0.4 \pm 1.2$ MeV and $20.7 \pm 1.6 \pm 2.5$ MeV for the central mass and the total (hadronic) width, respectively, which is in fair agreement with the above results of the CUSB and CLEO Collaborations. In the PDG tables [13], this enhancement is classified as a $b\bar{b}$ resonance, under the entry $\Upsilon(10580)$. However, in view of our results, we do not believe this enhancement to represent a resonance. Rather, the enhancement at 10.58 GeV suggests an accumulation of $B\bar{B}$ pairs in this invariant-mass region. Therefore, a description in terms of a wave function with a dominant $B\bar{B}$ component appears to be more adequate than assuming a pole in the scattering amplitude due to a supposed underlying $b\bar{b}$ state.

More than two decades ago, it naturally seemed obvious to associate the huge enhancement just above the $B\bar{B}$ threshold with the $\Upsilon(4S)$ state. Namely, the generally quite successful *Relativized quark Model* (RQM) by Godfrey and Isgur [42], employing the usual funnel-type confining potential, predicted the $\Upsilon(4S)$ state at 10.63 GeV, i.e., just 50 MeV too high. In view of the unpredictable threshold effects of the open-bottom decay channels at the time, this was a rather accurate prediction. However, the extensive tables of Godfrey and Isgur also contain an $\Upsilon(3D)$ state at 10.70 GeV. Why this state was not associated with the resonance at 10.684 GeV observed by the CLEO Collaboration [12], rather than classifying it as a presumable $b\bar{b}g$ hybrid, is a mystery to us. We conclude here that the *latter* state probably is the $\Upsilon(4S)$ resonance. Table 2 gives a compilation of the various results for the $B\bar{B}$ enhancement.

4.2 The $\Upsilon(4S)$ resonance

In Ref. [2], we found 10.77 GeV for the real part of the $4\,^3S_1$ $b\bar{b}$ resonance pole, in a multichannel calculation for scattering of open-bottom mesons This statement is actually not entirely correct, since $^3S_1$ and $^3D_1$ states mix, so that any resonance contains mixtures of all possible $^3S_1$ and $^3D_1$ states. Nevertheless, in Ref. [20] this mixing phenomenon was studied for charmonium, concluding that mixings are not very large. So we may say that the resonance at about 10.77 GeV is dominantly $4\,^3S_1$.

The bare spectrum for the HORSE contains a degenerate $4\,^3S_1/3\,^3D_1$ mass level at 10.873 GeV (see Eq. (13)). This level is then split into two resonances by the coupling to the decay channels, resulting in one state that is dominantly $3\,^3D_1$, with a small mass shift for the real part of the resonance pole, and one dominantly 4^3S_1 state, shifted quite considerably. We associate the

Collaboration	Interpretation	Mass (GeV)	Width (MeV)
RSE (this work)	nonresonant	–	–
CUSB [11]	$\Upsilon(4S)$	10.5774 ± 0.001	25 ± 2.5
CLEO [12]	$\Upsilon(4S)$	$10.5775 \pm 0.0007 \pm 0.004$	$20 \pm 2 \pm 4$
BABAR [1, 10]	$\Upsilon(10580)$	$10.5793 \pm 0.0004 \pm 0.0012$	$20.7 \pm 1.6 \pm 2.5$
PDG [13]	$\Upsilon(4S)$		20.5 ± 2.5

Table 2: Comparison of masses and widths for the enhancement at 10.58 GeV.

enhancement at 10.735 GeV found in this work with the latter resonance, and the bump at 10.867 GeV with the former one.

In Fig. 6 we show a detail of Fig. 1 for the invariant-mas interval 10.658–10.758 GeV, while in Table. 3 we compare our result to the available literature.

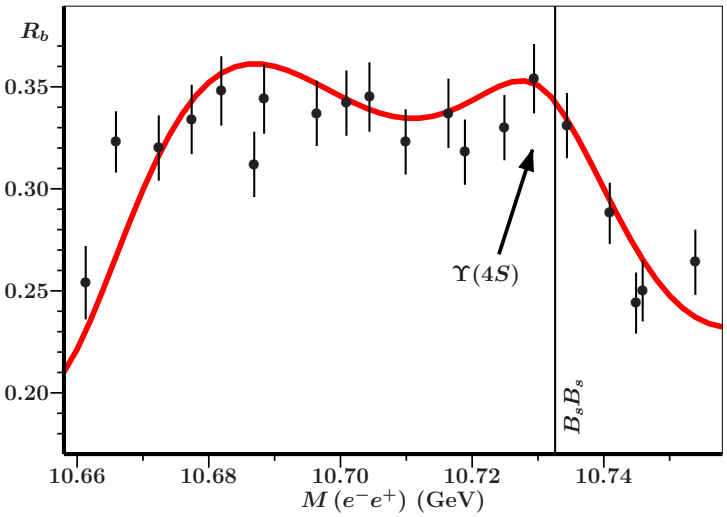

Figure 6: Detail of our result (—) in the $\Upsilon(4S)$ region, compared to the data (•) for hadron production in electron-positron annihilation published by the *BABAR* Collaboration [1]. We have baptized this figure the *elephit*, as it shows that even with a few parameters one can fit an elephant (J. von Neumann [43]).

Our central mass of the $\Upsilon(4S)$ (see Table 3) is more than 3 standard deviations higher than that of the CLEO Collaboration [12]. On the other hand, for the width we find a much smaller value than theirs. The reason for either discrepancy is simple. Namely, we have besides the resonance also a peaking nonresonant signal, which interferes with the $\Upsilon(4S)$. Hence, a substantial part of the enhancement does not belong to the resonance structure, which only corresponds to a very modest signal, almost coinciding with the $B_s\bar{B}_s$ threshold. Its effect is actually best seen just above this threshold, where it gives rise to the *trunk* of the elephant-like structure we baptized *elephit* (see the caption of Fig. 6). As a matter of fact, by moving the

Collaboration	Identification	Mass (GeV)	Width (MeV)
RSE (this work)	$\Upsilon(4S)$	10.735	38
CUSB [11]	–	–	–
CLEO [12]	$b\bar{b}g$	$10.684 \pm 0.010 \pm 0.008$	$131 \pm 27 \pm 23$
BABAR [1]	–	–	–
PDG [13]	–	–	–

Table 3: Comparison of masses and widths for the $\Upsilon(4S)$.

central mass position of the $\Upsilon(4S)$ to lower or higher masses, one can wiggle the trunk of the elephant (J. von Neumann [43]). Namely, from Eqs. (11,14), also the phase of the resonance depends on its central mass position.

4.3 The $\Upsilon(3D)$ and $\Upsilon(5S)$ resonances

The identification of the resonance at 10.845 GeV (CUSB) or 10.868 GeV (CLEO) and the resonance at 11.02 GeV (CUSB) or 11.019 GeV (CLEO) with the $\Upsilon(5S)$ and $\Upsilon(6S)$ states, respectively, is in conformity with the RQM [42] predictions at 10.88 GeV and 11.10 GeV, respectively. However, we rather identify these resonances with the $\Upsilon(3D)$ and $\Upsilon(5S)$ states,

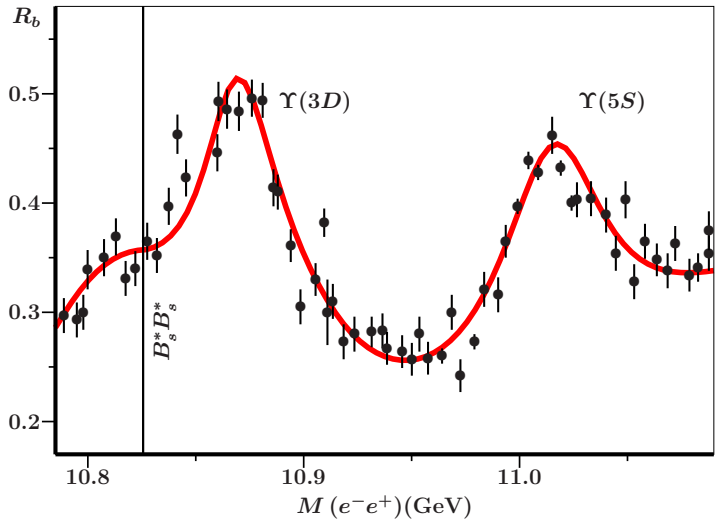

Figure 7: Detail of our result (—) for the $\Upsilon(3D)$ and $\Upsilon(5S)$ resonances, compared to the data (•) for hadron production in electron-positron annihilation published by the *BABAR* Collaboration [1]. The nonresonant contribution (—) is relatively large in this invariant-mass interval. One can read the mass of the $B_s^* \bar{B}_s^*$ threshold from the vertical line.

respectively. The reason is that, using a b mass of 4.724 GeV and an oscillator frequency of

$\omega = 0.19$ GeV [3], the RSE quenched $4S$, $3D$, and $5S$ $b\bar{b}$ states come out at 10.873 GeV, 10.873 GeV, and 11.253 GeV, respectively. Unquenching the bare bottomonium spectrum by inserting the open-bottom meson loops [2, 15] results in a multichannel scattering amplitude of the form given in Eq. (2), which via Eq. (1) also describes production processes. For both types of processes, resonance poles can be searched for by numerically determining the zeros of $D(\sqrt{s})$ in Eq. (2). Thus, we find that the $b\bar{b}$ bare states turn into resonances which for S states have central masses some 150–200 MeV below the unquenched masses, whereas the D states undergo mass shifts from a few MeV up to roughly 50 MeV. These mass shifts largely depend on the precise positions of the open-bottom thresholds. In Fig. 7 we show a detail of Fig. 1 for the invariant-mass interval 10.785–11.090 GeV, while in Tables 4 and 5 we compare our findings to those found in the literature. Our central mass for the $\Upsilon(10860)$ (see Table 4) is in good agreement with those

Collaboration	Identification	Mass (GeV)	Width (MeV)
RSE (this work)	$\Upsilon(3D)$	10.867	42
CUSB [11]	$\Upsilon(5S)$	10.845 ± 0.020	110 ± 15
CLEO [12]	$\Upsilon(5S)$	$10.868 \pm 0.006 \pm 0.005$	$112 \pm 17 \pm 23$
BABAR [1]	$\Upsilon(10860)$	10.876 ± 0.002	43 ± 4
PDG [13]	$\Upsilon(10860)$	10.865 ± 0.008	110 ± 13

Table 4: Comparison of masses and widths for the $\Upsilon(3D)$.

of the CUSB [11],CLEO [12], *BABAR* [1] Collaborations, and also with the PDG [13] value. As for the width of the $\Upsilon(10860)$, we find a much smaller value than CUSB, CLEO, and the PDG, which is nonetheless in excellent agreement with the very recent *BABAR* [1] value. However, on the experimental side there is a considerable systematic uncertainty with respect to the mass and width, due to the arbitrariness in the choice of the interfering background. Let us quote from the *BABAR* paper [1] itself (page 7):

> "The number of states is, a priori, unknown as are their energy dependencies. Therefore, a proper coupled channel approach including the effects of the various thresholds outlined earlier would be likely to modify the results obtained from our simple fit. As an illustration of the systematic uncertainties arising from the assumptions in our fit, a simple modification is to replace the flat nonresonant term by a threshold function at $\sqrt{s} = 2m_B$. This leads to a larger width (74 ± 4 MeV) and a lower mass (10.869 ± 0.002 GeV) for the $\Upsilon(10860)$."

The latter value for the width is significantly larger than ours, but the central mass is now in perfect agreement with our result.

Our central mass of the $\Upsilon(11020)$ (see Table 5) agrees well with those of CUSB, CLEO, and the PDG, but is several standard deviations larger than the result of *BABAR*. As for the width of the $\Upsilon(11020)$, we find a smaller value than CUSB and the PDG, agree with the CLEO result, and are six standard deviations away from the *BABAR* value. However, as we have just seen, the latter *BABAR* results depend quite sensitively on the choice of interfering background.

Collaboration	Identification	Mass (GeV)	Width (MeV)
RSE (this work)	$\Upsilon(5S)$	11.017	59
CUSB [11]	$\Upsilon(6S)$	11.02 ± 0.03	90 ± 20
CLEO [12]	$\Upsilon(6S)$	11.019 ± 0.005	$61 \pm 13 \pm 22$
BABAR [1]	$\Upsilon(11020)$	10.996 ± 0.002	37 ± 3
PDG [13]	$\Upsilon(11020)$	11.019 ± 0.008	79 ± 16

Table 5: Comparison of masses and widths for the $\Upsilon(5S)$.

4.4 The plateaux in R_b

In Ref. [1], the *BABAR* Collaboration observed two plateaux in R_b. The first one comes just below the $\Upsilon(4S)$, and is depicted in Fig. 6. As shown through our theoretical curve, we do not associate the data with a plateau, but rather with the back and the shoulders of an elephant. Also from Figs. 1 and 3 we seem to learn that neither the nonresonant contribution nor the resonance have a particularly flat behavior in the mass region delimited by the $B^*\bar{B}^*$ and $B_s\bar{B}_s$ thresholds. As for the nonresonant part, this mass interval constitutes a window for $B^*\bar{B}^*$ production, which signal in part "carries" the $\Upsilon(4S)$ resonance. Furthermore, the tail of the resonance interferes with the nonresonant contribution, leading to the shallow dip in between the elephant's back and shoulder.

However, the *BABAR* Collaboration also points at a second plateau, above the $\Upsilon(5S)$, which we have depicted in Fig. 8. Here, we indeed observe a flat pattern for R_b, which we assume to

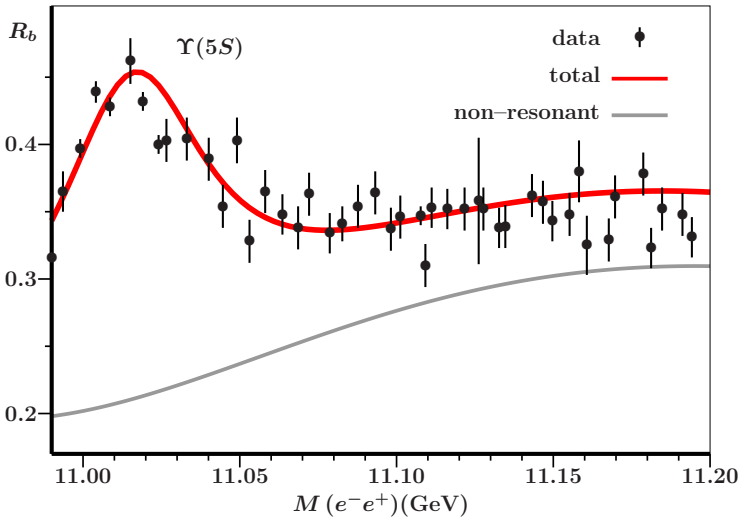

Figure 8: Detail of our result (—) for the $\Upsilon(5S)$ resonance and the "plateau", compared to the data (•) for hadron production in electron-positron annihilation published by the *BABAR* Collaboration [1]. The nonresonant contribution (—) is relatively large and flat in this invariant-mass interval.

be the result of a slowly rising nonresonant contribution and the tail of the $\Upsilon(5S)$ resonance. It actually lends further credit to our picture for open-bottom production in electron-positron annihilation. Namely, the slowly rising behavior with increasing invariant mass of the nonresonant contribution stems from the small value of the r_0 parameter for BX. This is completely in line with the result discussed in Sect. 3.4 and summarized in Fig. 5.

5 Proposed experiment

A possible confirmation of the here observed phenomena could come from an analysis over the same set of data, but with additional criteria for event selection:

1. $B\bar{B}$ events for invariant masses above the BB^* threshold.

2. Two-meson events containing just one B meson for invariant masses above the $B^*\bar{B}^*$ threshold.

As explained in the preceding sections, we expect that above the BB^* threshold the cross sections of the type-1 events decrease very fast for increasing invariant masses. For the type-2 events, we expect a similar behavior above the $B^*\bar{B}^*$ threshold, up to invariant masses of about 10.9 GeV. From 10.9 GeV upwards, we expect the latter cross section to rise, as with increasing invariant masses more and more open-bottom BX channels open, where X represents any excited B meson. The effective pair-creation radius of this type of channels is small, of the order of 0.221 fm, which implies that the corresponding signals reach their maxima roughly 300 MeV above threshold. A further broadening of the line shapes may stem from the hadronic widths of the X mesons. If it turns out to be possible in the analysis of the data sample to continue up to the $\Lambda_b\bar{\Lambda}_b$ threshold, one might even observe a glimpse of the $b\bar{b}$ $4D$ resonance (see below).

As far as spectroscopy is concerned, just above the $\Lambda_b\bar{\Lambda}_b$ threshold we expect for this channel a similar pattern as has been observed for $\Lambda_c\bar{\Lambda}_c$ [4]. However, unlike in the $\Lambda_c\bar{\Lambda}_c$ case, where the bare states lie reasonably far away from threshold, the $\Lambda_b\bar{\Lambda}_b$ threshold at 11.2404 ± 0.0022 GeV [13] comes just below the bare $4D/5S$ state at 11.253 GeV [3], which could cause a sharp dip in the cross section at that invariant mass [18,32]. However, it is not clear to us where the $4D$ resonance will lie precisely. It may even end up just below the $\Lambda_b\bar{\Lambda}_b$ threshold, since the partner $5S$ resonance at 11.017 GeV is pulled down by as much as 236 MeV, which is more than the usual mass shift of S-wave resonances with respect to the corresponding bare states [2]. However, the $6S$ state, which is probably also pulled down towards the $\Lambda_b\bar{\Lambda}_b$ threshold, will produce a clear signal at roughly 11.4 GeV, so well below the $\Sigma_b\bar{\Sigma}_b$ threshold.

6 Summary and Conclusions

Using a BW approximation to an amplitude developed for the description of meson-pair production in electron-positron annihilation [14], we obtained a satisfactory description of the R_b data very recently published by the *BABAR* Collaboration [1]. The approximation spoils the property of the exact amplitude that it satisfies Watson's theorem for relating production and scattering [16]. However, the approximation allowed us to unravel some of the missing ingredients for a complete description of hadron production in electron-positron annihilation. A very important feature here is that the formalism allows for a well-defined separation in resonant and nonresonant contributions.

We have found important new ingredients for modeling quarkonia, in particular $b\bar{b}$ systems. In the first place, depending on whether the phenomenon that is most clearly exhibited in Fig. 4 is correctly interpreted by us, it seems that open-bottom pair production for small kinetic energies is dominated by initial light-quark production, rather than by the heavy $b\bar{b}$ propagator. An almost exact factor of 4 between the couplings for $e^-e^+ \to (b\bar{n})(n\bar{b})$ (n for u or d) and the couplings for $e^-e^+ \to (b\bar{s})(s\bar{b})$ remains to be explained. Secondly, we found that the universal frequency for strong interactions ω plays an important role in relating phases between nonresonant and resonant contributions to the total production amplitudes (see Eqs. (11) and (14)), and also in interrelating interaction radii (see Eq. (20)). Throughout the present work we have used the value $\omega = 0.190$ GeV, which has been optimized in Ref. [3] and kept fixed ever since. Finally, we found that the distributions of Ref. [17] for $^3P_0$ quark-pair creation are useful for the construction of workable form factors for open-bottom meson-pair production.

Relation (16) for the couplings of the three resonances $\Upsilon(4S)$, $\Upsilon(3D)$ and $\Upsilon(5S)$ to the $b\bar{b}$ propagator is a clear indication for the here proposed spectroscopic identification of these resonances. For the $\Upsilon(4S)$ we have obtained a central resonance mass of 10.735 GeV and a width of 38 MeV.

Acknowledgments

We are most grateful for the precise measurements and data analyses of the *BABAR* Collaboration, which made the present analysis possible. We also thank Dr. K. P. Khemchandani for many useful discussions. This work was supported in part by the *Fundação para a Ciência e a Tecnologia* of the *Ministério da Ciência, Tecnologia e Ensino Superior* of Portugal, under contract CERN/FP/83502/2008.

References

[1] B. Aubert [BaBar Collaboration], *Measurement of the $e^+e^- \to b\bar{b}$ cross section between $\sqrt{s}$ = 10.54-GeV and 11.20-GeV*, Phys. Rev. Lett. **102**, 012001 (2009) arXiv:0809.4120 [hep-ex]].

[2] E. van Beveren, C. Dullemond, and G. Rupp, *Spectra and strong decays of $c\bar{c}$ and $b\bar{b}$ states*, Phys. Rev. D **21**, 772 (1980) [Erratum-ibid. D **22**, 787 (1980)].

[3] E. van Beveren, G. Rupp, T. A. Rijken, and C. Dullemond, *Radial spectra and hadronic decay widths of light and heavy mesons*, Phys. Rev. D **27**, 1527 (1983).

[4] G. Pakhlova *et al.* [Belle Collaboration], *Observation of a near-threshold enhancement in the $e^+e^- \to \Lambda_c^+\Lambda_c^-$ cross section using initial-state radiation*, Phys. Rev. Lett. **101**, 172001 (2008) [arXiv:0807.4458 [hep-ex]].

[5] E. van Beveren and G. Rupp, *Production of hadron pairs in e^+e^- annihilation near the K^+K^-, $D\bar{D}$, $B\bar{B}$ and $\Lambda_c^+\Lambda_c^-$ thresholds*, Phys. Rev. D **80**, 074001 (2009) [arXiv:0908.0242 [hep-ph]].

[6] B. Aubert *et al.* [BABAR Collaboration], *Observation of a broad structure in the $\pi^+\pi^- J/\psi$ mass spectrum around 4.26-GeV/c^2*, Phys. Rev. Lett. **95**, 142001 (2005) [arXiv:hep-ex/0506081].

[7] B. Aubert [BaBar Collaboration], *Study of the $\pi^+\pi^- J/\psi$ mass spectrum via Initial-State Radiation at BaBar*, arXiv:0808.1543 [hep-ex].

[8] E. van Beveren and G. Rupp, *The $X(4260)$ and possible confirmation of $\psi(3D)$, $\psi(5S)$, $\psi(4D)$, $\psi(6S)$ and $\psi(5D)$ in $J/\psi\pi\pi$*, arXiv:0904.4351 [hep-ph].

[9] E. van Beveren and G. Rupp, *Interference effects in the $X(4260)$ signal*, Phys. Rev. D **79**, 111501R (2009) [arXiv:0905.1595 [hep-ph]].

[10] B. Aubert [BaBar Collaboration], *A measurement of the total width, the electronic width, and the mass of the $\Upsilon(10580)$ resonance*, Phys. Rev. D **72**, 032005 (2005) [arXiv:hep-ex/0405025].

[11] D. M. J. Lovelock *et al.* [CUSB Collaboration], *Masses, widths, and leptonic widths of the higher upsilon resonances*, Phys. Rev. Lett. **54**, 377 (1985).

[12] D. Besson *et al.* [CLEO Collaboration], *Observation of new structure in the e^+e^- cross section above the $\Upsilon(4S)$*, Phys. Rev. Lett. **54**, 381 (1985).

[13] C. Amsler *et al.* [Particle Data Group Collaboration], *Review of Particle Physics*, Phys. Lett. B **667**, 1 (2008).

[14] E. van Beveren and G. Rupp, *Relating multichannel scattering and production amplitudes in a microscopic OZI-based model*, Ann. Phys. **323**, 1215 (2008) [arXiv:0706.4119].

[15] E. van Beveren and G. Rupp, *Reconciling the light scalar mesons with Breit-Wigner resonances as well as the quark model*, Int. J. Theor. Phys. Group Theor. Nonlin. Opt. **11**, 179 (2006) [arXiv:hep-ph/0304105].

[16] K. M. Watson, *The effect of final state interactions on reaction cross-sections*, Phys. Rev. **88**, 1163 (1952).

[17] E. van Beveren, *Coupling constants and transition potentials for hadronic decay modes of a meson*, Z. Phys. C **21**, 291 (1984) [arXiv:hep-ph/0602246].

[18] E. van Beveren, and G. Rupp, *Meson-meson interactions and Regge propagators*, Ann. Phys. **324**, 1620 (2009) [arXiv:0809.1149 [hep-ph]].

[19] C. Dullemond, T. A. Rijken, E. van Beveren and G. Rupp, *On The influence of hadronic decay on the properties of hadrons*, in proceedings of *VIth Warsaw Symposium on Elementary Particle Physics, Kazimierz, Poland, 30 May - 3 Jun 1983*, pp 257-262.

[20] E. van Beveren, C. Dullemond and T. A. Rijken, *On the influence of hadronic decay on the properties of hadrons*, Z. Phys. C **19**, 275 (1983).

[21] E. van Beveren, T. A. Rijken, K. Metzger, C. Dullemond, G. Rupp and J. E. Ribeiro, *A low lying scalar meson nonet in a unitarized meson model*, Z. Phys. C **30**, 615 (1986) [arXiv:0710.4067 [hep-ph]].

[22] H. Harari, *A dual absorptive model for dips in inelastic hadron processes*, Phys. Rev. Lett. **26**, 1400 (1971).

[23] P. Dasgupta and S. Biswas, *Duality, Unitarity And Exotic Peaks*, J. Phys. G **2**, L167 (1976).

[24] E. van Beveren and G. Rupp, *The spectrum of scalar-meson nonets in the Resonance-Spectrum Expansion*, in Proceedings of the *Workshop on scalar mesons and related topics, honoring the 70th birthday of Michael Scadron* (SCADRON 70), Lisbon, Portugal, 11-16 Feb 2008, AIP Conf. Proc. **1030**, 219 (2008) [arXiv:0804.2573 [hep-ph]].

[25] N. Brambilla *et al.* [Quarkonium Working Group], *Heavy quarkonium physics*, CERN Yellow Report, CERN-2005-005, arXiv:hep-ph/0412158.

[26] E. Eichten, K. Gottfried, T. Kinoshita, K. D. Lane and T. M. Yan, *Interplay of confinement and decay in the spectrum of charmonium*, Phys. Rev. Lett. **36**, 500 (1976).

[27] E. Eichten, K. Gottfried, T. Kinoshita, K. D. Lane and T. M. Yan, *Charmonium: 1. The Model*, Phys. Rev. D **17**, 3090 (1978) [Erratum-ibid. D **21**, 313 (1980)].

[28] E. J. Eichten, K. Lane and C. Quigg, *Charmonium levels near threshold and the narrow state* $X(3872) \to \pi^+\pi^- J/\psi$, Phys. Rev. D **69**, 094019 (2004) [arXiv:hep-ph/0401210].

[29] E. van Beveren and G. Rupp, *Observed $D_s(2317)$ and tentative $D(2100\text{-}2300)$ as the charmed cousins of the light scalar nonet*, Phys. Rev. Lett. **91**, 012003 (2003) [arXiv:hep-ph/0305035].

[30] E. van Beveren and G. Rupp, *Continuum bound states K-long, $D_1(2420)$, $D_{s1}(2536)$ and their partners K-short, $D_1(2400)$, $D^*_{sJ}(2463)$*, Eur. Phys. J. C **32**, 493 (2004) [arXiv:hep-ph/0306051].

[31] E. van Beveren and G. Rupp, *New BABAR state* $D_{sJ}(2860)$ *as the first radial excitation of the* $D^*_{s0}(2317)$, Phys. Rev. Lett. **97**, 202001 (2006) [arXiv:hep-ph/0606110].

[32] E. van Beveren, X. Liu, R. Coimbra, and G. Rupp, *Possible* $\psi(5S)$, $\psi(4D)$, $\psi(6S)$, *and* $\psi(5D)$ *signals in* $\Lambda_c\bar{\Lambda}_c$, Europhys. Lett. **85**, 61002 (2009) [arXiv:0809.1151 [hep-ph]].

[33] D. S. Hwang and D.-W. Kim, *Mass of* $D^*_{sJ}(2317)$ *and Coupled Channel Effect*, Phys. Lett. B **601**, 137 (2004) [arXiv:hep-ph/0410301]; D. S. Hwang and D. W. Kim, *Mass shift of D/sJ(2317)* by coupled channel effect*, J. Phys. Conf. Ser. **9**, 63 (2005).

[34] G. Goldhaber *et al.*, *D and D* meson production near 4-Gev in* e^+e^- *annihilation*, Phys. Lett. B **69**, 503 (1977).

[35] E. van Beveren, *Recoupling matrix elements and decay*, Z. Phys. C **17**, 135 (1983) [arXiv:hep-ph/0602248].

[36] D. V. Bugg, *An alternative fit to Belle mass spectra for* $D\bar{D}$, $D^*\bar{D}^*$ *and* $\Lambda_C\bar{\Lambda}_C$, J. Phys. G **36**, 075002 (2009) [arXiv:0811.2559 [hep-ph]].

[37] J. Wel, *Least squares fitting of an elephant*, ChemTech, February (1975), 128.

[38] S. Prell [BaBar Collaboration], *CP Violation at BaBar:* $\sin(2\beta)$, talk presented at the B-Factory Symposium in recognition of the achievements of PEP-II and BABAR, Stanford, 27 October 2008.

[39] C. and J. de Brunhoff, *L'Histoire de Babar le petit éléphant*, (1931, Paris: Éditions du Jardin des Modes, Groupe des Publications Condé Nast).

[40] G. Orwell, *Animal Farm: A Fairy Story*, (1945, London: Secker and Warburg).

[41] W. Blümel and U. Heinz, *Pion multiplicity distribution in anti-proton - proton annihilation at rest*, Z. Phys. C **67**, 281 (1995) [arXiv:hep-ph/9409343].

[42] S. Godfrey and N. Isgur, *Mesons in a relativized quark model with chromodynamics*, Phys. Rev. D **32**, 189 (1985).

[43] F. Dyson, *A meeting with Enrico Fermi*, Nature 427, 297 (2004).